

Noise temperature spectrum of hot electrons in semiconductor superlattices

C. Wang, J. C. Cao, and Chao Zhang

Citation: *Journal of Applied Physics* **105**, 013717 (2009); doi: 10.1063/1.3065523

View online: <http://dx.doi.org/10.1063/1.3065523>

View Table of Contents: <http://scitation.aip.org/content/aip/journal/jap/105/1?ver=pdfcov>

Published by the AIP Publishing

Articles you may be interested in

[A study of vertical and in-plane electron mobility due to interface roughness scattering at low temperature in InAs/GaSb type-II superlattices](#)

J. Appl. Phys. **114**, 053712 (2013); 10.1063/1.4817088

[In-plane and growth direction electron cyclotron effective mass in short period InAs/GaSb semiconductor superlattices](#)

J. Appl. Phys. **110**, 043720 (2011); 10.1063/1.3627171

[Optically detected cyclotron resonance studies of \$\text{In}_x\text{Ga}_{1-x}\text{N}_y\text{As}_{1-y}/\text{GaAs}\$ quantum wells sandwiched between type-II AlAs/GaAs superlattices](#)

J. Appl. Phys. **101**, 073705 (2007); 10.1063/1.2714776

[Silicon quantum dot superlattices: Modeling of energy bands, densities of states, and mobilities for silicon tandem solar cell applications](#)

J. Appl. Phys. **99**, 114902 (2006); 10.1063/1.2203394

[Effective mass enhancement of two-dimensional electrons in a one-dimensional superlattice potential](#)

Appl. Phys. Lett. **76**, 3600 (2000); 10.1063/1.126719



Launching in 2016!
The future of applied photonics research is here

AIP | APL
Photonics

Noise temperature spectrum of hot electrons in semiconductor superlattices

C. Wang,¹ J. C. Cao,^{1,a)} and Chao Zhang^{2,b)}

¹State Key Laboratory of Functional Materials for Informatics, Shanghai Institute of Microsystem and Information Technology, Chinese Academy of Sciences, 865 Changning Road, Shanghai 200050, People's Republic of China

²School of Engineering Physics, University of Wollongong, New South Wales 2522, Australia

(Received 1 September 2008; accepted 30 November 2008; published online 15 January 2009)

The small signal response and thermal noise spectra in miniband superlattice are investigated. The properties of hot electron differential mobility, velocity fluctuation, and noise temperature are determined around a stationary condition. The field and frequency dependent drift velocity, electron energy, effective mass, and electron temperature are obtained. At low frequencies, noise temperature increases rapidly with the electric field. Our calculated noise temperatures for miniband superlattice are in good agreement with the experimental results, with the sample thickness estimated to be around 4 μm . © 2009 American Institute of Physics. [DOI: 10.1063/1.3065523]

I. INTRODUCTION

Electron transport in semiconductor superlattices can reveal important information on quantum effects, nonlinear effects, and the role of various scatterings. Since the seminal work of Esaki and Tsu,¹ many interesting dynamical behaviors have been observed and analyzed in biased semiconductor superlattices. These behaviors include negative differential velocity (NDV),^{2,3} nonlinear effects,^{4,5} formation of electrical field domain,⁶ self-sustained current oscillation,⁷⁻⁹ and chaos.¹⁰ Recently, nonlinear dynamics involving electron transport in semiconductor superlattice driven by an intense terahertz electromagnetic irradiation has been a central focus of theoretical and experimental studies.¹¹⁻¹⁸ Keay *et al.*¹³ observed the photon-assisted tunneling and oscillatory dependence of the photon induced currents on terahertz electric field. It was reported that current through a biased GaAs/AlAs superlattice is reduced when exposed to an intense terahertz field.¹⁴ Moreover, terahertz emission¹⁵ and possible terahertz gain¹⁶ can be achieved in miniband superlattices. The recent development in terahertz quantum cascade lasers is based on the nonlinear transport and electron-phonon interaction in superlattices.¹⁹⁻²¹ These studies are motivated by the promising properties offered by superlattices for terahertz optoelectronic device applications.

Despite the rapid progress in fundamental sciences of superlattices and its application in telecommunications and optoelectronics, some key issues regarding dynamical electron transport in miniband superlattices remain unsolved. One of the unsolved problems is the small signal response and electronic noise. It was observed that the noise temperature in superlattices grows exponentially with the field amplitude in the low frequency regime.²² To date the mechanism of this unusually large noise spectrum is still poorly understood. The understanding of this problem is crucial to developing devices operating in terahertz frequency. As a stochastic signal superimposed to the output signal of the

device, electronic noise should be reduced because of the limitation on device sensitivity. From the knowledge of electronic noise, we can extensively understand the microscopic feature of electron transport related to scattering processes in superlattices. The detailed knowledge of differential mobility, velocity fluctuation, and noise temperature in terahertz frequency range is of fundamental importance in understanding electron transport in nanostructures and the performances of devices based on miniband superlattices. Because the noise temperature contains information on the microscopic properties (such as scattering process) of nanostructures, it can also be used as a sensitive diagnostic tool to detect impurities, defects, and interface states.²³ The frequency dependent electrical properties can also provide useful information to improve the performance and reliability of devices based on miniband superlattice.

The purpose of this work is to present an understanding on the small signal response of miniband superlattices. The kinetic coefficients, such as the differential mobility, the velocity fluctuation, and the noise temperature in terahertz frequency regime, are calculated under various dc biases. We shall show that the rapid increase of the noise temperature with the field amplitude has the origin of scattering-mediated electron mobility and is due to the interplay of slow decrease in velocity fluctuation and rapid decreasing of mobility around the NDV regime.

II. ELECTRON TRANSPORT IN SUPERLATTICES

Let us consider a n -doped semiconductor superlattice with spatially homogeneous miniband in a stationary condition under the influence of an electric field E along the growth direction (i.e., z axis). The electrons in the superlattice can travel freely in the x - y plane but are subject to a periodic potential in the z direction. We assume that only the transverse ground state and the longitudinal lowest miniband need to be taken into account. Thus we have a quasi-one-dimensional system with the energy dispersion described by a one-dimensional wave vector k_z . Within the tight-binding approximation, the electron state in the superlattice miniband is

^{a)}Electronic mail: jccao@mail.sim.ac.cn

^{b)}Electronic mail: czhang@uow.edu.au.

$$\varepsilon(k_z) = \frac{\Delta}{2} [1 - \cos(k_z d)], \quad (1)$$

where Δ is the width of the lowest miniband and d is the superlattice period.

Under a uniform electric field E applied parallel to the z axis, the electrons are accelerated by the field and scattered by disorders and phonons, leading to an overall drift motion and heating of the electron system. The macroscopic average state of the electron system can be described by the momentum and energy balance equations in the form^{3,24}

$$\frac{dv_d}{dt} = \frac{eE}{m_z^*} - \nu_v(h_e)v_d, \quad (2)$$

$$\frac{dh_e}{dt} = eEv_d - \nu_e(h_e)(h_e - h_{e0}). \quad (3)$$

Here, v_d is the average drift velocity of electrons along the z axis, h_e is the average electron energy, m_z^* is the electron's average effective mass along the z axis, and $\nu_v(h_e)$ and $\nu_e(h_e)$ are energy dependent momentum and energy relaxation frequencies, respectively. h_{e0} is the thermal equilibrium energy.

The transport state of the electron system is described by the center-of-mass momentum p_d and the relative electron temperature T_e , while the ensemble-averaged quantities v_d , h_e , and m_z^* are functions of p_d and T_e , i.e.,

$$v_d = \frac{\Delta d}{2\hbar} \alpha_1(T_e) \sin\left(\frac{p_d d}{\hbar}\right), \quad (4)$$

$$\frac{1}{m_z^*} = \frac{\Delta d^2}{2\hbar^2} \alpha_1(T_e) \cos\left(\frac{p_d d}{\hbar}\right), \quad (5)$$

$$h_e = \frac{\Delta}{2} \left[1 - \alpha_1(T_e) \cos\left(\frac{p_d d}{\hbar}\right) \right], \quad (6)$$

where $\alpha_1(T) = \langle \cos(k_z d) \rangle$. The average is over the Brillouin zone in the superlattice direction at the lattice temperature T . From Eqs. (5) and (6) the ensemble-averaged effective mass of electron is given as $m_z^* = M_0 / (1 - 2h_e / \Delta)$ with $M_0 = 2\hbar^2 / \Delta d^2$.

For a given superlattice structure where electrons are in a steady state under a uniform electric field, the average drift velocity v_d , average electron energy h_e , and electron effective mass m_z^* can be obtained by solving the balance equations (2) and (3) with $dv_d/dt=0$ and $dh_e/dt=0$, respectively. The electron temperature T_e and center-of-mass momentum p_d can be calculated from Eqs. (4) and (5).

When a weak time-dependent field $\delta E(t) = \delta E \exp(i2\pi\nu t)$ is superimposed to the dc electric field E , the electron differential mobility can be calculated according to the linear response theory

$$\mu(\nu) = e \int_0^\infty \alpha_x(t) \exp(-i2\pi\nu t) dt, \quad (7)$$

where $\alpha_x(t)$ is the linear response function of the average electron velocity to an arbitrary variation in time of the electric field.

The response function can be calculated using the balance equation approach under stationary and homogenous conditions.²⁵ The spectral density of velocity fluctuation is written in the form

$$S_{vv}(\nu) = 4 \int_0^\infty C_{vv}(t) \cos(2\pi\nu t) dt, \quad (8)$$

with $C_{vv}(t)$ as the correlation function of drift velocity fluctuations. In linear response theory, correlation function $C_{vv}(t)$ is determined by the eigenvalues of the response matrix, the variance of velocity fluctuations $\langle \delta v^2 \rangle$, and the covariance of velocity-energy fluctuations $\langle \delta v \delta h_e \rangle$.

III. NOISE TEMPERATURE SPECTRUM IN MINIBAND SUPERLATTICES

The frequency dependent electron noise of superlattice originates from velocity fluctuation of electrons during their motion across the superlattice miniband. The fluctuation is caused by the interaction of electron with phonons and impurities, which have a stochastic character both in time and space.²⁶ The electron noise can be experimentally measured in high frequency range based on the frequency dependent noise temperature $T_n(\nu)$. Theoretically, noise temperature $T_n(\nu)$ is defined by a generalized Nyquist relation

$$T_n(\nu) = \frac{e S_{vv}(\nu)}{4k_B \operatorname{Re}[\mu(\nu)]}, \quad (9)$$

where k_B is the Boltzmann constant and $\operatorname{Re}[\mu(\nu)]$ is the real part of the electron differential mobility. From the definition, the noise temperature should be always positive and depends on the spectral density of velocity fluctuation and real part of differential mobility. Actually, the real part of differential mobility can be negative in a certain frequency range when the electric field is in the NDV region. This leads to the failure of the definition of noise temperature. The analysis of the noise temperature in the condition of negative differential mobility in bulk materials can be found in Ref. 26.

The procedure of calculating the noise temperature is as follows. First, we solve balance equations to obtain the electric field dependence of average electron velocity v_d , average energy h_e , electron effective mass m_z^* , and electron temperature T_e for miniband superlattice. Second, the response function and correlation function are determined using these stationary state parameters. When calculating the momentum and energy relaxation rates ν_v and ν_e , electron scattering by charged impurities, acoustic phonons, and optical phonons has been included.²⁴ By making use of these results, we solved Eqs. (2) and (3) to obtain the stationary state quantities. In our calculation, the superlattice period is $d=15$ nm and the electron density is $n=1.07 \times 10^{18} \text{ cm}^{-3}$.

In Fig. 1 we show the calculated average electron velocity v_d , average energy h_e , effective mass of electrons m_z^* , and electron temperature T_e as functions of electric field E for the superlattice with miniband width $\Delta=70$ meV at lattice temperatures of $T=4.2$, 77, and 300 K, respectively. The average drift velocity v_d exhibits a peak velocity v_p at a critical electric field E_c . This is a characteristic of hot electron on superlattices. This hot electron characteristic is more pronounced

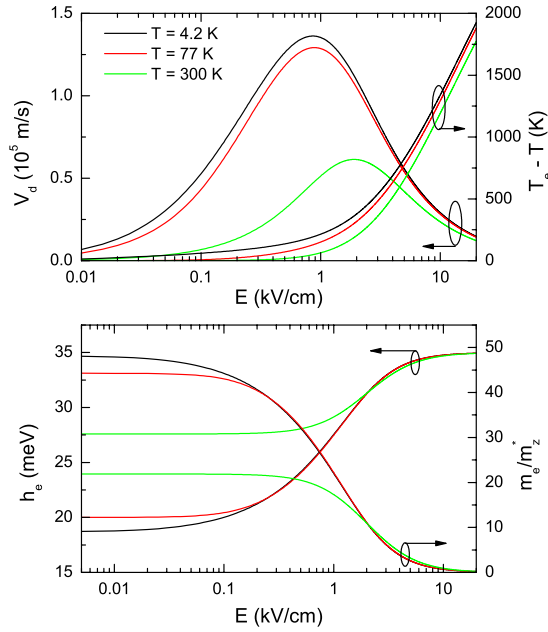


FIG. 1. (Color online) Field dependent average electron drift velocity v_d , electron temperature $T_e - T$, average electron energy h_e , and inverse effective mass m_e/m_z^* for hot electrons in miniband superlattice with $\Delta = 70$ meV at lattice temperatures of $T = 4.2$, 77, and 300 K, respectively.

at low lattice temperatures than at high temperatures. With the increase of electric field, v_d enters the NDV regime. The peak of drift velocity shifts to a high electric field region with the increase of lattice temperature. The origin of NDV in superlattice is the Bragg reflection of Bloch electron in the boundary of Brillouin zone. This mechanism is different from that of bulk materials, such as GaN and InN, where the NDV is mainly caused by intervalley transfer of electrons to upper valleys as the electric field increases.²⁷ The behavior of electron temperature T_e at different lattice temperatures is also presented in Fig. 1(a). The electron average energy h_e and inverse effective mass m_z^* are depicted in Fig. 1(b). The average electron energy h_e increases almost linearly in the low electric field regime. When the electric field is above 7 kV/cm, h_e saturate toward $\Delta/2$, which is due to the significant increase in the electron temperature with increasing electric field.

The spectra of the real part of the hot electron differential mobility $\text{Re}[\mu(\nu)]$ are shown in Fig. 2(a) under different electric fields. For the cases of $E = 0.08$ and 0.4 kV/cm, the spectra of $\text{Re}[\mu(\nu)]$ exhibit a Lorentzian shape. For the other cases the spectra of $\text{Re}[\mu(\nu)]$ exhibit a plateau in low frequency region from 0.01 to 0.2 THz depending on the electric field, a peak at the intermediate frequencies about 0.2–3 THz, and a decay in the high frequency region above 3 THz. The spectra of $\text{Re}[\mu(\nu)]$ decrease in the low frequency range with the increase of electric fields, which are due to the reduction in $\alpha_x(t)$ with an increase in electric field in the region $t < 0.3$ ps and the appearance of negative tails. When the electric field is above the critical field E_c and NDV shows up in the $v_d - E$ relation, the values of $\text{Re}[\mu(\nu)]$ are reduced to negative in the low frequency region.

The spectral density of the velocity fluctuations $S_{vv}(\nu)$ is reported in Fig. 2(b) for a superlattice with miniband width

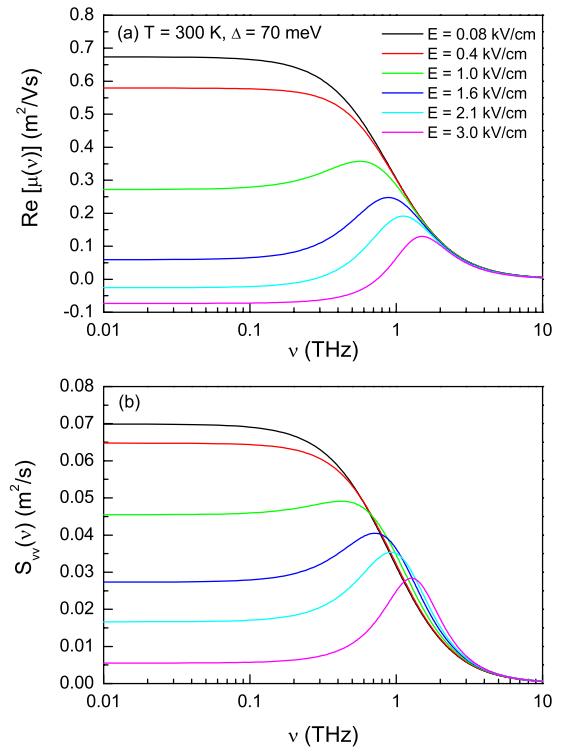


FIG. 2. (Color online) (a) The real part of the differential mobility $\text{Re}[\mu(\nu)]$ for hot electron in miniband superlattice and (b) the spectral density of velocity fluctuation. The electric fields are $E = 0.08$, 0.4, 1.0, 1.6, 2.1, and 3.0 kV/cm, respectively.

of $\Delta = 70$ meV. The spectral density has a Lorentzian shape in low electric fields due to the simple exponential behavior of correlation function. The decrease in initial values and the appearance of negative tails as well as oscillating behavior in $C_{vv}(t)$ with the increase of electric field lead to the decrease in $S_{vv}(\nu)$ at low frequency range. As follows from the comparison of Figs. 2(a) and 2(b), the frequency dependent correlation function $S_{vv}(\nu)$ exhibits a rather similar behavior to $\text{Re}[\mu(\nu)]$. It is worth noting that $S_{vv}(\nu)$ is always positive in contrary to the spectrum of $\text{Re}[\mu(\nu)]$, which is negative at low frequencies when biased in the NDV region.

The results of noise temperature $T_n(\nu)$ for electrons in superlattice are shown in Fig. 3 with $T = 300$ K and $\Delta = 70$ meV. In the region below the critical field E_c (i.e., $E = 0.08$, 0.4, 1.0, and 1.6 kV/cm), $\text{Re}[\mu(\nu)]$ and $T_n(\nu)$ are both positive in the whole frequency range. For these electric fields, the spectra of $T_n(\nu)$ exhibit two plateaus in the low and high frequency regions, respectively. The noise temperature spectrum shows a transition from low frequency plateau to high frequency plateau. For electric fields above the critical field E_c (i.e., $E = 2.1$ and 3.0 kV/cm), in the low frequency region $\text{Re}[\mu(\nu)]$ becomes negative leading to the negative value of $T_n(\nu)$ (this region is shown in the inset of Fig. 3). This feature can be interpreted as the possibility for the devices based on miniband superlattice to become an active element under suitable conditions. The decrease of noise temperature with frequency is mainly due to the rapid decrease of velocity fluctuation at high frequencies. Below the critical field E_c , as the electric field increases, the noise tem-

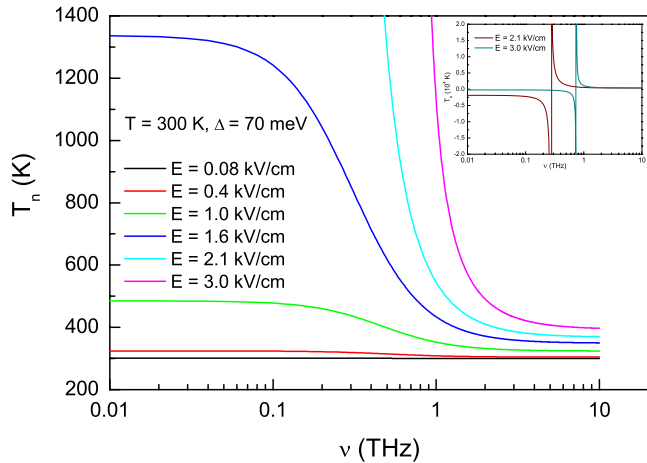


FIG. 3. (Color online) Noise temperature spectra of hot electrons in miniband superlattice with $\Delta=70$ meV and $T=300$ K. The electric fields are $E=0.08, 0.4, 1.0, 1.6, 2.1$, and 3.0 kV/cm, respectively. The inset shows the noise temperature spectra at high fields.

perature increases in the whole frequency range. This also implies the presence of hot electrons in superlattice miniband.

The low frequency noise temperature spectrum as a function of electric field is presented in Fig. 4. It is observed that with the increase of electric field, the noise temperature increases rapidly. The inset in Fig. 4 is the experimental results of voltage dependent noise temperature for hot electron in miniband superlattice (reproduced from Ref. 22). These experimental results were measured at 4 GHz by inserting the superlattice sample into microstrip lines and microwave connectors. This frequency falls in the region of the first plateau of the noise temperature shown in Fig. 3. It can be seen that the calculated noise temperatures are in good agreement with that of the experimental results. To make a quantitative comparison between the calculated and measured spectra, it is necessary to estimate the strength of the electric field in the sample. The threshold voltage of the experimental spectra is at 0.2 V, while the threshold electric field from the

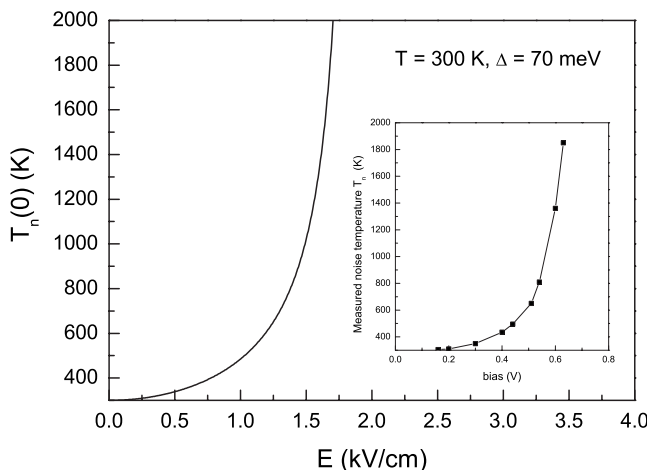


FIG. 4. Noise temperature spectrum in low frequency as function of electric field for superlattice with miniband width $\Delta=70$ meV and lattice temperature $T=300$ K. The inset indicates the experimental results of voltage dependent noise temperature of miniband superlattice. The experimental results are reproduced from Ref. 22.

calculation is around 0.5 kV/cm. The required sample thickness for achieving a quantitative agreement between the calculated and measured spectra can be estimated as follows: $t=(0.2 \text{ V})/(500 \text{ V/cm})=4 \text{ } \mu\text{m}$. The thickness of the superlattice region in Ref. 22 is $1 \text{ } \mu\text{m}$. The thickness of the contact layers is unknown. Our analysis indicates that the contact layer thickness is around $1\text{--}2 \text{ } \mu\text{m}$.

IV. CONCLUSIONS

In summary, we have studied the hot electron noise temperature spectrum in miniband superlattice. The quantities describing hot electron transport in stationary state, such as the average electron velocity, the average energy, the electron temperature, and the inverse effective mass, have been determined. The frequency dependence of the differential mobility and the velocity fluctuation of hot electrons in miniband superlattice are obtained. Based on these results, the frequency and field intensity dependence of the noise temperature originating from velocity fluctuations of hot electron moving in the superlattice is determined. Our result agrees well with the experiment.

ACKNOWLEDGMENTS

This work was supported by the National Basic Research Program of China (973 Program, Grant No. 2007CB310402), the National Natural Science Foundation of China (Grant No. 60721004), the Shanghai Municipal Commission of Science and Technology (Grant Nos. 06dj14008 and 06CA07001), and the Australian Research Council.

- ¹L. Esaki and R. Tsu, IBM J. Res. Dev. **14**, 61 (1970).
- ²A. Sibille, J. F. Palmier, H. Wang, and F. Mollot, *Phys. Rev. Lett.* **64**, 52 (1990).
- ³X. L. Lei, N. J. M. Horing, and H. L. Cui, *Phys. Rev. Lett.* **66**, 3277 (1991).
- ⁴A. Wacker, *Phys. Rep.* **357**, 1 (2002).
- ⁵G. Platero and R. Aguado, *Phys. Rep.* **395**, 1 (2004).
- ⁶H. T. Grahn, R. J. Haug, W. Müller, and K. Ploog, *Phys. Rev. Lett.* **67**, 1618 (1991).
- ⁷E. Schomburg, T. Blomeier, K. Hofbeck, J. Grenzer, S. Brandl, I. Lingott, A. A. Ignatov, K. F. Renk, D. G. Pavel'ev, Yu. Koschurinov, B. Ya. Melzer, V. M. Ustinov, S. V. Ivanov, A. Zhukov, and P. S. Kop'ev, *Phys. Rev. B* **58**, 4035 (1998).
- ⁸J. C. Cao and X. L. Lei, *Phys. Rev. B* **59**, 2199 (1999).
- ⁹Z. Z. Sun, X. R. Wang, S. Yin, J. P. Cao, Y. P. Wang, and Y. Q. Wang, *Appl. Phys. Lett.* **87**, 182110 (2005).
- ¹⁰O. M. Bulashenko and L. L. Bonilla, *Phys. Rev. B* **52**, 7849 (1995).
- ¹¹L. L. Bonilla and H. T. Grahn, *Rep. Prog. Phys.* **68**, 577 (2005).
- ¹²A. A. Ignatov, K. F. Renk, and E. P. Dodin, *Phys. Rev. Lett.* **70**, 1996 (1993).
- ¹³B. J. Keay, S. J. Allen, Jr., J. Galán, J. P. Kaminski, K. L. Campman, A. C. Gossard, U. Bhattacharya, and M. J. W. Rodwell, *Phys. Rev. Lett.* **75**, 4098 (1995).
- ¹⁴X. L. Lei, *J. Appl. Phys.* **82**, 718 (1997).
- ¹⁵Y. Shimada, K. Hirakawa, M. Odnobliudov, and K. A. Chao, *Phys. Rev. Lett.* **90**, 046806 (2003).
- ¹⁶T. Hyart, N. V. Alexeeva, A. Leppänen, and K. N. Alekseev, *Appl. Phys. Lett.* **89**, 132105 (2006).
- ¹⁷C. Zhang, *Appl. Phys. Lett.* **78**, 4187 (2001).
- ¹⁸C. Zhang, *Phys. Rev. B* **66**, 081105(R) (2002).
- ¹⁹R. Köhler, A. Tredicucci, F. Beltram, H. E. Beere, E. H. Linfield, A. G. Davies, D. A. Ritchie, R. C. Iotti, and F. Rossi, *Nature (London)* **417**, 156 (2002).

- ²⁰B. S. Williams, S. Kumar, Q. Qin, Q. Hu, and J. L. Reno, *Appl. Phys. Lett.* **88**, 261101 (2006).
- ²¹B. S. Williams, S. Kumar, H. Callebaut, Q. Hu, and J. L. Reno, *Appl. Phys. Lett.* **83**, 5142 (2003).
- ²²E. Dutisseuil, A. Sibille, J. F. Palmier, V. Thierry-Mieg, M. de Murcia, and E. Richard, *J. Appl. Phys.* **80**, 7160 (1996).
- ²³L. Varani, P. Houlet, J. C. Vaissière, J. P. Nougier, E. Starikov, V. Gruzinskis, P. Shiktorov, L. Reggiani, and L. Hlou, *J. Appl. Phys.* **80**, 5067 (1996).
- ²⁴J. C. Cao, H. C. Liu, and X. L. Lei, *Phys. Rev. B* **61**, 5546 (2000).
- ²⁵V. Gruzinskis, E. Starikov, P. Shiktorov, L. Reggiani, M. Saraniti, and L. Varani, *Semicond. Sci. Technol.* **8**, 1283 (1993).
- ²⁶P. Shiktorov, V. Gruzinskis, E. Starikov, L. Reggiani, and L. Varani, *Phys. Rev. B* **54**, 8821 (1996).
- ²⁷E. Starikov, P. Shiktorov, V. Gruinskis, L. Varani, J. C. Vaissière, C. Palermo, and L. Reggiani, *J. Appl. Phys.* **98**, 083701 (2005).